

[Click for updates](#)

## International Journal of Geographical Information Science

Publication details, including instructions for authors and subscription information:

<http://www.tandfonline.com/loi/tgis20>

### An alternative approach to transverse and profile terrain curvature

Patrik Krebs<sup>a</sup>, Markus Stocker<sup>b</sup>, Gianni Boris Pezzatti<sup>a</sup> & Marco Conedera<sup>a</sup>

<sup>a</sup> Insubric Ecosystems Group, Research Unit Community Ecology, Swiss Federal Research Institute WSL, Bellinzona, Ticino, Switzerland

<sup>b</sup> Research Group of Environmental Informatics, Department of Environmental Science, University of Eastern Finland, Kuopio, Northern Savonia, Finland

Published online: 18 Mar 2015.

To cite this article: Patrik Krebs, Markus Stocker, Gianni Boris Pezzatti & Marco Conedera (2015) An alternative approach to transverse and profile terrain curvature, International Journal of Geographical Information Science, 29:4, 643-666, DOI: [10.1080/13658816.2014.995102](https://doi.org/10.1080/13658816.2014.995102)

To link to this article: <http://dx.doi.org/10.1080/13658816.2014.995102>

PLEASE SCROLL DOWN FOR ARTICLE

Taylor & Francis makes every effort to ensure the accuracy of all the information (the "Content") contained in the publications on our platform. However, Taylor & Francis, our agents, and our licensors make no representations or warranties whatsoever as to the accuracy, completeness, or suitability for any purpose of the Content. Any opinions and views expressed in this publication are the opinions and views of the authors, and are not the views of or endorsed by Taylor & Francis. The accuracy of the Content should not be relied upon and should be independently verified with primary sources of information. Taylor and Francis shall not be liable for any losses, actions, claims, proceedings, demands, costs, expenses, damages, and other liabilities whatsoever or howsoever caused arising directly or indirectly in connection with, in relation to or arising out of the use of the Content.

This article may be used for research, teaching, and private study purposes. Any substantial or systematic reproduction, redistribution, reselling, loan, sub-licensing, systematic supply, or distribution in any form to anyone is expressly forbidden. Terms &



## An alternative approach to transverse and profile terrain curvature

Patrik Krebs<sup>a\*</sup>, Markus Stocker<sup>b</sup>, Gianni Boris Pezzatti<sup>a</sup> and Marco Conedera<sup>a</sup>

<sup>a</sup>Insubric Ecosystems Group, Research Unit Community Ecology, Swiss Federal Research Institute WSL, Bellinzona, Ticino, Switzerland; <sup>b</sup>Research Group of Environmental Informatics, Department of Environmental Science, University of Eastern Finland, Kuopio, Northern Savonia, Finland

(Received 14 August 2014; final version received 30 November 2014)

Terrain curvature is one of the most important parameters of land surface topography. Well-established methods used in its measurement compute an index of plan or profile curvature for every single cell of a digital elevation model (DEM). The interpretation of these outputs may be delicate, especially when selected locations have to be analyzed. Furthermore, they involve a high level of simplification, contrasting with the complex and multiscalar nature of the surface curvature itself. In this paper, we present a new method to assess vertical transverse and profile curvature combining real-scale visualization and the possibility to measure these two terrain derivatives over a large range of scales. To this purpose, we implemented a GIS tool that extracts longitudinal and transverse elevation profiles from a high-resolution DEM. The performance of our approach was compared with some of the most commonly used methods (ArcMap, Redlands, CA, USA; ArcSIE, Landserf) by analyzing the terrain curvature around charcoal production sites in southern Switzerland. The different methods produced comparable results. While conventional methods quickly summarize terrain curvature in the form of a matrix of values, they involve a loss of information. The advantage of the new method lies in the possibility to measure and visualize the shape and size of the curvature, and to obtain a realistic representation of the average curvature for different subsets of spatial points. Moreover, the new method makes it possible to control the conditions in which the index of curvature is calculated.

**Keywords:** landforms; concavity/convexity; DEM; elevation profiles; geomorphometry; morphometric variables

### 1. Introduction

Since at least the 1960s, terrain curvature has been recognized as one of the most important parameters of land surface topography (Curtis *et al.* 1965, Speight 1968). As such, it is now considered and measured with great care by specialists in many scientific fields and is included and presented as a salient aspect of landscapes in a countless number of databases, management reports, and scientific publications (Moore *et al.* 1991, Wilson and Gallant 2000, Huggett and Cheeseman 2002, Hengl and Reuter 2009).

In differential geometry, curvature ( $\kappa$ ) is a measure of how curved a curve is, that is, of how far it is from being a straight line (Abate and Tovenia 2012). As already described around 1671 in Newton's *De methodis serierum et fluxionum* (Knoebel *et al.* 2007), for a plane curve, the curvature can be expressed as the inverse of the radius of the osculating circle that locally approximates the curve at a given point.

---

\*Corresponding author. Email: [patrik.krebs@wsl.ch](mailto:patrik.krebs@wsl.ch)

In geomorphology, terrain curvature is a continuous and multiscale surface phenomenon that can be defined as the rate of change of a first derivative, such as slope gradient or aspect, in a particular direction (Wilson and Gallant 2000, Romstad and Etzelmüller 2012). In reality, this rate is never constant, which makes calculating the curvature surprisingly difficult. The most established measures of curvatures are those defined by the principal planes intersecting the topographic surface (Wilson and Gallant 2000, Peckham 2011). In particular, *plan curvature* is the curvature in the horizontal plane, while *profile curvature* is the curvature in the vertical plane oriented in the direction of the steepest slope. Less acknowledged are the *tangential curvature*, calculated in the oblique plane perpendicular to the slope line (Schmidt *et al.* 2003), and the *streamline curvature*, measuring the rate at which the flow direction changes along the streamline (Peckham 2011, Evans 2013, Minár *et al.* 2013). The matter is more complicated when we consider the number of terms with a similar meaning (De Smith *et al.* 2007). For instance, *planform curvature*, *contour curvature*, *horizontal curvature*, and *transverse curvature* sometimes have been used as synonymous of *plan curvature*; usually *vertical curvature* has a similar meaning to *profile curvature*, and *rotor curvature* and *flow path curvature* are synonyms of *streamline curvature*. For their part, *longitudinal curvature* and *cross-sectional curvature* are quite similar to *profile curvature* and *tangential curvature*, respectively, even if their functions are clearly different (Wood 1996, De Smith *et al.* 2007, Jenness 2013). Moreover, some of these expressions have been used in confusingly different ways in literature (Schmidt *et al.* 2003, Florinsky 2011, Jenness 2013), and inconsistencies exist regarding definitions and equations (Porres de la Haza and Pardo Pascual 2002, Blaga 2012, Jenness 2013). As observed by several authors (e.g., Hart and Sagan 2007, Jenness 2013), for a given point on the terrain, there is theoretically an infinite number of ways in which the curvature can be measured. Shary (1995, see also Shary *et al.* 2002) proposed a classification system that recognizes and integrates 12 different types of curvature. The system was further extended by other authors (Schmidt *et al.* 2003, Dong *et al.* 2008). Despite this variety of terms and procedures, modern geomorphometry continues to rely largely on techniques developed decades ago, and curvature is always reported and represented as an index, that is, as a single value for every square cell of the digital elevation model (DEM) (Evans 1972, 1980, Krcho 1973, Zevenbergen and Thorne 1987, Moore *et al.* 1991, Florinsky and Kuryakova 1996, Wood 1996, 2009b). In GIS analysis, for instance, the curvature is a common geomorphometric terrain derivative, extracted and calculated from DEM and then stored in the form of grid, raster, or matrix indices. This conventional curvature index offers undeniable advantages, such as simplicity and a direct relationship with DEM cells. Furthermore, it is implemented in most GIS software packages, which explains its success as one of the most important parameters of land surface topography. However, it also has some limitations, especially when the land surface curvature must be depicted in detail and analyzed at a variety of scales (Wood 1996, Shi *et al.* 2007). Specifically, curvature  $\kappa$  values are strongly dependent on scale, so that the effect of DEM resolution has to be considered with great care (Shary *et al.* 2005). Any matrix of topographic attributes is necessarily a simplification of the irregular and curvilinear forms of land surface (Schmidt *et al.* 2003, Erskine *et al.* 2007). Owing to this simplification, to the lack of clarity concerning the unit of measurement, and to the differences in the usage of plus and minus signs, it is very difficult to mentally imagine the true form of the terrain represented by these indices. In addition, due to the narrowness of the moving window taken into consideration, the resulting values may be sensitive to errors and noise (i.e., outliers and striping artifacts) in light detection and ranging (LiDAR)-derived elevation data and may fail to represent the

general trend of the curvature (Schmidt *et al.* 2003, Erskine *et al.* 2007, Sofia *et al.* 2013), although solutions have been proposed to mitigate these problems (Shary *et al.* 2002, Albani and Klinkenberg 2003). Florinsky (1998) found that the accuracy of curvature  $\kappa$  values may be poor especially when calculated on flat terrains. Albani *et al.* (2004) showed that the use of a moving window larger than  $3 \times 3$  allows a substantial reduction in the effect of elevation errors on terrain derivatives but can lead to an excessive generalization of the topographic surface.

One may ask why plan or profile terrain curvatures should be reduced to a single number. Would it not be more effective to report the convexity and concavity in the transverse or longitudinal direction through two simple curved lines (' $\cap$ ' and ' $\cup$ ') rather than through two  $\kappa$  values? In this respect, an elevation profile may be a good way of illustrating the curvature of the terrain at a given point, especially when it is centered at that point, oriented in transverse or longitudinal direction and conceived with the difference in altitude from the point (vertical axis) versus the horizontal distance from the point (horizontal axis).

In this paper, we first review the main existing methods of curvature extraction from a DEM and then present an alternative approach for measuring and visualizing terrain curvature in the form of self-explanatory profiles. This approach led to the development of a tool that automatically extracts, represents, measures, and statistically assesses the two fundamental elevation profiles from DEM: the transverse elevation profile (TEP) and the longitudinal elevation profile (LEP). The first is a cross profile along the mean orientation of the contour line, while the second is a profile following the line of maximum slope, although the procedure of orientation is independent from these two lines (see Figure 1 and Section 3.1 explaining the alternative approach). Finally, we evaluate the new approach comparing it with some of the most commonly used ones by applying all of them to the challenging test case of the study of terrain curvature around wood charcoal production sites (CPS) in selected areas in the Canton Ticino, Southern Switzerland.

We discuss the following research questions in particular:

- Are there significant differences between our method and conventional methods in characterizing terrain curvature around CPS?
- What advantages and disadvantages does this new approach have in comparison to conventional methods, in terms of terrain curvature assessment and visualization?
- Are curvature profiles a good way of assessing the relationship between CPS and terrain curvature?

## 2. Methods for assessing terrain curvature

Commonly used approaches for assessing terrain curvature and related algorithms mostly use a moving window of  $3 \times 3$  cells and calculate the curvature of the central raster cell by referring to the elevation of its eight neighbors (Corripio 2003, Tarolli *et al.* 2012, Jenness 2013). The nine elevation data points of the window are first approximated by a type of polynomial surface (Evans 1980, Zevenbergen and Thorne 1987, Florinsky 1998, Hurst *et al.* 2012, Jenness 2013) from which the morphometric terrain parameters are derived (e.g., curvature). This is the method currently used in many commercial GIS software packages (e.g., ArcMap from Esri, Redlands, CA, USA; TNTmips from MicroImages, Lincoln, NE, USA; RiverTools from Rivix, Broomfield, CO, USA), ArcGIS extensions (e.g., ET Surface, ET SpatialTechniques, Faerie Glen, Pretoria, South Africa; DEM

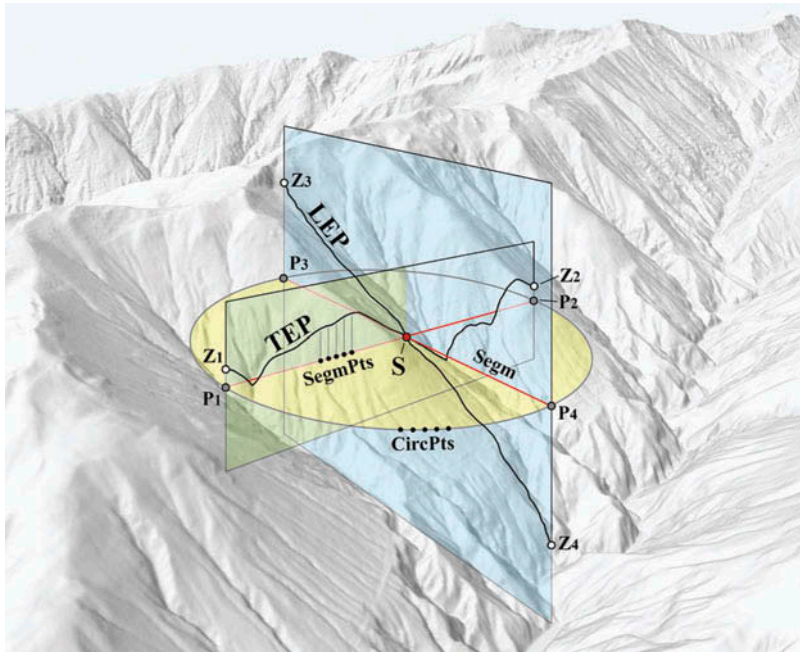


Figure 1. The transverse elevation profile (TEP) and the longitudinal elevation profile (LEP) calculated starting from a site (S). To obtain these two vertical profiles, we draw a horizontal circle centered on the site with diameter equal to the desired profile segment length (Segm). The orientation of the TEP is given by the pair of diametrically opposed circle points (P1 and P2) minimizing the difference in altitude when projected on the DEM (Z1 and Z2), while the orientation of the LEP is given by the pair of opposed circle points (P3 and P4) maximizing the difference in altitude on the DEM (Z3 and Z4).

Surface Tools, Jenness Enterprises, Flagstaff, AZ, USA), and open-source GIS software (e.g., QGIS, QGIS Development Team, International Developer Community; SAGA GIS, SAGA User Group Association, International Developer Community; PCRaster, PCRaster R&D team, Utrecht, Netherlands). With this predominant method, the neighborhood size is determined by the pixel size (Shi *et al.* 2007, Gao *et al.* 2012), so that the calculation of the curvature at larger spatial scales presupposes the resampling of the DEM. This, in turn, results in a lowered resolution with a consequent loss of a large part of the elevation data.

Only a few software packages attempt to overcome this problem by allowing the user to select the neighborhood size independently of the DEM resolution. This is the case, for instance, with ArcSIE, an extension of ESRI's ArcMap®, which calculates the eight elevation values on the edge of a square or circular neighborhood through bilinear interpolation (Shi *et al.* 2007, Shi 2013). Other software, such as Landserf (cfr. 3dMapper), offers a more advanced method that allows the user to define the neighborhood size by selecting the odd number of pixels that defines the side of the moving window (Wood 2009a). The software then approximates the surface of the DEM inside the window by fitting a bivariate quadratic function to all elevation points. Note that the same method has been implemented also in GRASS (see the Jo Wood's software overview chapter in Hengl and Reuter 2009, at page 333). The drawback of this approach is that computation times tend to become very long (Gao *et al.* 2012). Furthermore, no software provides a report of the goodness of fit, so that it is very difficult to evaluate how well polynomial functions



represent the DEM surface. Most existing software packages also fail to properly indicate the units of the curvature values. For instance, in the ArcGIS 10.1 desktop help library and in the ArcSIE user's guide, the units of the curvature are not clearly defined (Shi 2013). Probably the most commonly used curvature units are degrees per hundred meters (Evans 1980) and radians per hundred meters (Wilson and Gallant 2000, Jenness 2013), but other units, such as radians per foot or radians per meter, are also mentioned (Porres de la Haza and Pardo Pascual 2002, Milevski 2007, Smith 2012). According to Reuter and Nelson (in Hengl and Reuter 2009, p. 278), ESRI software products (e.g., ArcGIS) calculate curvature in radians/100 m (Table 1). Concerning Landserf, its user's guide states that curvature is measured as a dimensionless ratio (Wood 2009a, p. 81, cfr., Prasicek *et al.* 2014). The sign of the curvature index is problematic too. Usually in earth sciences convexity is positive and concavity is negative, while in mathematics the signs may be reversed (Shary 2008). Because earth sciences and mathematics cannot be divorced, this can lead to a lack of agreement about the meaning of positive and negative values (Blaga 2012, Minár *et al.* 2013). Contrary to what is stated by Hengl and Reuter (2009), there are software packages that disregard the rule about the positive curvature sign of convex surface shapes (see, for instance, ArcMap and Landserf in Table 1).

In conclusion, despite its undeniable advantages with regard to simplicity, the direct relationship with DEM cells, and its implementation in most GIS software packages, the conventional curvature index approach shows some limitations, especially when specific points on the land surface need to be analyzed in depth and at a variety of scales (Wood 1996).







### 3. Proposed approach

#### 3.1. The Elevation profiler



We developed a GIS tool (hereafter referred to as the *Elevation profiler*) for the extraction of the two fundamental elevation profiles (TEP and LEP) starting from a DEM and a point shapefile. These two elevation profiles represent the intersection of vertical planes with the DEM surface (Figure 1). The tool is conceived as a VBA macro that can be added and run from the visual basic editor in ArcMap (see Appendix A in the supplementary electronic materials for details).

Input data and initial parameters required by the *Elevation profiler* are a DEM, a shapefile with the Cartesian coordinates of at least one site (see S on Figure A.2), the diameter (D) and the desired number of points on the circle (CircPts) and on the profile segment (SegmPts). For each site, the tool first builds a circle of regularly spaced points around each given site. Then it searches for the pair of diametrically opposed points on the circle that minimize the absolute difference of altitude when projected on the DEM (Figures 1 and A.2). The identified pair of opposed points (P1, P2) represents the endpoints of the transverse profile segment (TEP). In contrast, the pair of opposed circle points maximizing the absolute difference in altitude (P3, P4) defines the longitudinal profile segment (LEP). Thanks to this procedure, the resulting longitudinal and transverse profile segments respect the general configuration of topography around the site without depending only on a terrain attribute measured at one single point. In particular, LEP orientation is not dependent on the direction of the maximum slope gradient measured at the site, but is instead related to the overall flow direction in the circle determined by the profile diameter (Figure A.4), while TEP orientation is related to the overall direction of the contour lines in the same circle (Figure A.5). It follows that the TEP and LEP are oblique to each other and not necessarily perpendicular. Despite being completely

Table 1. Plan (or transverse) and profile curvature in the four tested geomorphometric methods (ArcMap, ArcSIE, Landserf, and Elevation profiler and Curvature visualizer).

Method	Terms and descriptions	Equations and sources			Unit
ArcMap	<i>Plan curve</i> : the curvature of the surface perpendicular to the slope direction. Planform curvature influences convergence and divergence of flow.	$2(DH^2 + EG^2 - FGH) / (G^2 + H^2)$ in Zevenbergen and Thorne (1987, p. 50, <i>planform curvature</i> ); $-2(bd^2 + ae^2 - cde) / (d^2 + e^2)$ in Wood (1996, p. 87, <i>cross-sectional curvature</i> ); see also Schmidt <i>et al.</i> (2003), Blaga (2012) and Jenness (2013).	-		radians/100LU
	<i>Profile curve</i> : the curvature of the surface in the direction of slope. Profile curvature affects the acceleration and deceleration of flow and, therefore, influences erosion and deposition.	$-2(DG^2 + EH^2 + FGH) / (G^2 + H^2)$ in Zevenbergen and Thorne (1987, p. 50); $-2(ad^2 + be^2 + cde) / (d^2 + e^2)$ in Wood (1996, p. 87, <i>longitudinal curvature</i> ); see also Schmidt <i>et al.</i> (2003), Blaga (2012), and Jenness (2013).	+		
ArcSIE	<i>Planform curvature</i> : measures the shape of the slope surface in the horizontal (cross-slope) direction.	Information on equations is not available. We used the Zevenbergen–Thorne algorithm (as recommended by ArcSIE) and the floating neighborhood method based on the circular shape. See Zevenbergen and Thorne (1987), Shi <i>et al.</i> (2007), and Shi (2013).	-		not specified
	<i>Profile curvature</i> : measures the shape of the slope surface in the vertical (up-and-down) direction.		-		



Landserf	<i>Plan curvature</i> : intersecting with the XY plane. Describes the rate of change of aspect in plan.	$200(bd^2 + ae^2 - cde) / (e^2 + d^2)^{1.5}$ in Wood (1996, p. 85); $-(q^2r - 2pqs + p^2t) / (p^2 + q^2)^{3/2}$ in Shary <i>et al.</i> (2002, p. 13); cfr. Schmidt <i>et al.</i> (2003, p. 800, <i>contour curvature</i> ); see also Evans (1979), Blaga (2012) and Jenness (2013).	+		dimensionless ratio
	<i>Profile curvature</i> : intersecting with the plane of the Z-axis and aspect direction. Describes the rate of change of slope in profile.	$-200(ad^2 + be^2 + cde) / (e^2 + d^2)(1 + d^2 + e^2)^{1.5}$ in Wood (1996, p. 85); $-(p^2r + 2pqs + q^2t) / ((p^2 + q^2)(1 + p^2 + q^2)^{3/2})$ in Shary <i>et al.</i> (2002, p. 13, <i>vertical curvature</i> ); cfr. Schmidt <i>et al.</i> (2003, p. 800); see also Evans (1979), Blaga (2012), and Jenness (2013).	-		radians/100LU
Elevation profiler and Curvature visualizer	<i>Transverse curvature</i> : is the curvature in the middle of a vertical elevation profile centered on the site and oriented so as to minimize the difference in altitude between its two endpoints.		+		
	<i>Profile curvature</i> : is the curvature in the middle of a vertical elevation profile centered on the site and oriented so as to maximize the difference in altitude between its two endpoints.	$100(f''(x) / (1 + (f'(x))^2)^{3/2})$ Cfr. Zevenbergen and Thorne (1987, p. 50), Mortimer (2005, p. 110).	+		

Note: From the left to the right, we present the terms used in the software interfaces, the main descriptions furnished, the equations, the main bibliographic sources, the signs adopted for concavity, the typical computation time, and the units of the curvature values (where LU is the unit of length).

different from the D-infinity routing, our procedure avoids the limitations related to some widely used algorithms, such as the Steepest Descent and the Deterministic 8 (Peucker and Douglas 1975, O'Callaghan and Mark 1984, Tarboton 1997, Hengl and Reuter 2009). The TEP represents the transverse curvature well since it always starts and ends at the same altitude, whereas the LEP portrays slope and curvature. The longitudinal curvature can be easily obtained by subtracting the mean slope line from the LEP (see Figure A.3 for details). The precision of the TEP and LEP orientation is highly dependent on the number of CircPts defined; we recommend to set at least 360 CircPts. Similarly, the number of points on the profile segment (SegmPts) will determine the level of detail of the elevation data on the profiles.

### 3.2. The Curvature visualizer

The outputs of the *Elevation profiler* are further processed with R (R Core Team 2013) for an in-depth analysis of the LEP and TEP curvatures. In particular, we use a specific R script (hereafter referred to as the *Curvature visualizer*) to perform the following steps for each considered site:

- calculate an n-degree polynomial that best approximates the elevation profile;
- calculate the coefficient of determination ( $R^2$ ) to evaluate the goodness of fit of the polynomial function;
- derive the curvature index ( $\kappa$  for  $x = 0$ ) in radians per hundred meters from this function;
- display, in the same plot, the DEM profile, the fitting function, and the osculating circle representing the curvature;
- write the calculated data in two tables that summarize  $\kappa$  and  $R^2$  results, respectively;
- compile a pdf file that presents the curvature profiles of all processed sites.

Finally, the elevation profiles are rotated and averaged in order to obtain different types of mean TEP or LEP curvature profiles.

## 4. Materials and methods

### 4.1. Experimental design

We developed our experimental design in order to test the suitability of the proposed approach using the CPS in Canton Ticino, Southern Switzerland. CPS are places where the transformation of wood into charcoal through traditional methods of carbonization (e.g., earth-covered heaps) was achieved one or more times in the past. Typically, CPS display a modified surface terrain, more specifically, a sort of platform with a flat and elliptical-shaped surface (with a longest diameter from 4 to 20 m) upon which an earth mound kiln (a neat pile of wood covered with insulating material) was built and, in turn, used in the carbonization process. This flat oval area is bounded upwardly by an excavation and is supported downwardly by an embankment or a simple dry-stone wall, resulting in a cut into the hillslope (Figure 2) (Rennie 1997, Ludemann *et al.* 2004). The particular needs of wood concentration, water availability, wind protection, soil thickness, and charcoal transportation reported in the literature (Svedelius 1875, Toffenetti 1993) combined with knowledge of the typical workflow in CPS lead to the hypothesis that CPS are not randomly distributed in the territory but are strategically placed in a network of

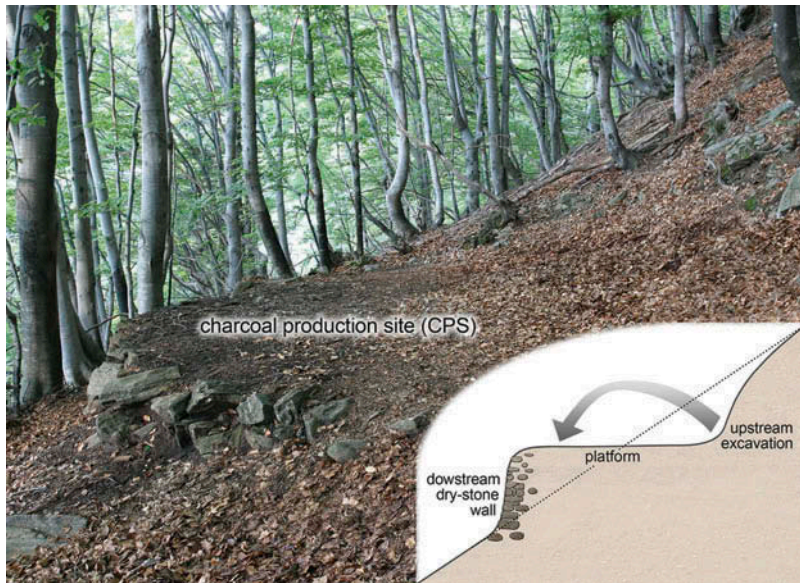


Figure 2. Typical structure of a CPS. The platform is formed by a simple cut and fill method. The back is dug out of the hillslope and the earth thrown forward to build up the front. The height of the back excavation and of the front bank depends upon the slope. Charcoal burners usually built these terraces in a short time by using simple tools (shovel, pickaxe) and exploiting the materials present on the spot (earth and stones).

suitable sites. Therefore, we expect that CPS terrain curvatures are significantly different from terrain curvatures of random points (RP).

To test this hypothesis, we exploited our systematic inventory of 1070 CPS in three geographically separated and geomorphologically different areas in Canton Ticino, which cover an area of 16.3 km<sup>2</sup> in total (Figure 3, Table 2). In all three areas, the nearest-neighbor ratio of CPS is significantly less than 1 ( $P < 0.001$ ), indicating that there is a tendency toward clustering. CPS aggregation is particularly marked in Muggio (nearest-neighbor ratio = 0.73), quite evident in Morobbia (0.81), and scarcely noticeable in Arbedo (0.91). The inventory was conducted from April 2009 to November 2011 through a field survey consisting in systematically exploring the whole study area on foot and georeferencing, by means of a GPS receiver with submeter accuracy (Trimble GeoXT), the identified CPS. In order to create a reference set to compare with the 1070 mapped CPS, we generated a sample of 1000 RP for each study area using the 'create random points' of ArcGIS (ERSI<sup>®</sup>). We forced a 10-m minimum horizontal distance between RP since the horizontal distance between CPS is almost never less than 10 m.

#### 4.2. Terrain curvature assessment

We obtained, for the three study areas, a high-resolution elevation model consisting of a LiDAR DEM with a pixel size of 2 m (see 'swissALTI3D' at [www.swisstopo.ch](http://www.swisstopo.ch)).

Plan and profile terrain curvature of CPS and RP were then assessed with the well-established methods provided by ArcMap, ArcSIE, and Landserf. These were compared to the vertical transverse and profile curvature calculated with the new method proposed

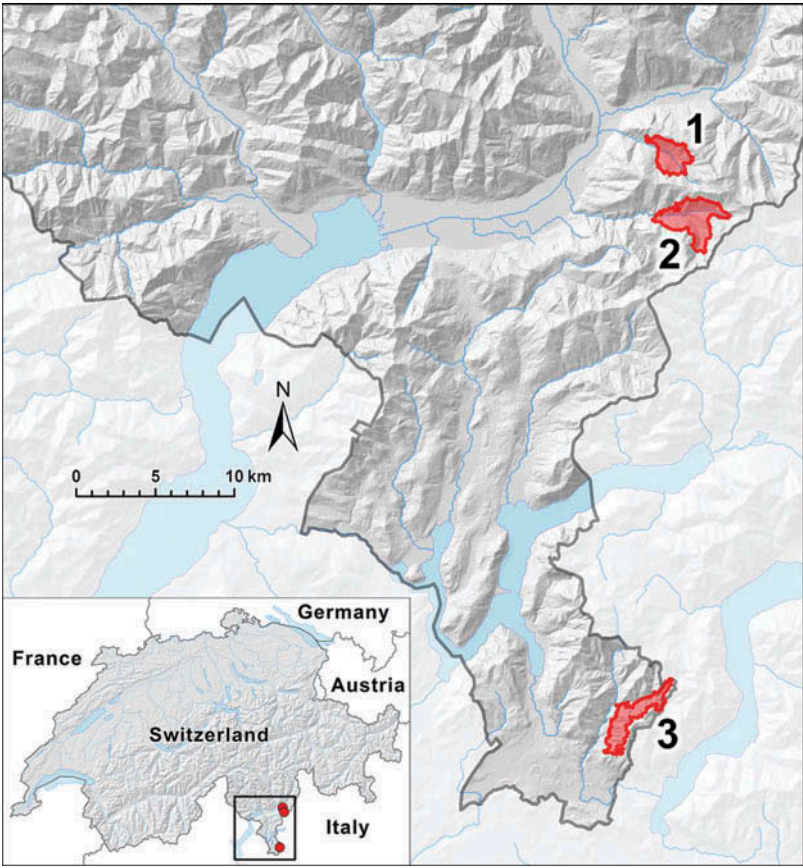


Figure 3. Location of the three study areas in southern Switzerland: Arbedo (1), 9° 5' 39", 46° 11' 54"; Morobbia (2), 9° 6' 37", 46° 9' 43"; Muggio (3), 9° 3' 9", 45° 52' 45". Latitudes and longitudes refer to the centroid of the polygon.

Table 2. Main characteristics of the three study areas.

	General data			Altitude			Slope		Aspect			
	No. CPS	Area (km <sup>2</sup> )	Forest (%)	Min	Max	Mean	Max	Mean	North (%)	East (%)	South (%)	West (%)
Arbedo	347	3.92	94.75	652.9	1539.4	1141.6	68.3	35.0	34.3	7.6	25.8	32.2
Morobbia	376	7.13	83.39	744.8	1804.9	1258.6	71.8	33.9	38.2	11.9	20.7	29.2
Muggio	347	5.22	89.66	538.2	1065.8	771.8	64.4	32.2	37.6	7.9	14.2	40.3

in this paper (*Elevation profiler* and *Curvature visualizer*). We defined neighborhood size as referring to the side of the moving window in ArcMap and Landserf, the diameter of the circular neighborhood in ArcSIE, and the profile segment length in the new method. In order to explore and compare the behavior of the curvature index over a large range of spatial scales, all calculations were repeated for a neighborhood size ranging from the minimum possible size up to 1000 m. In ArcMap, this required multiple resampling of the high-resolution LiDAR DEM to obtain a set of DEM covering all the requested cell sizes.

Plan and profile curvature were then calculated by analyzing all resampled DEMs with the basic  $3 \times 3$  moving window.

In ArcSIE, calculations were performed using the Zevenbergen–Thorne method with a circular neighborhood ranging from 10 to 1000 m in size.

In order to reduce computation time, in Landserf it was necessary to resample the LiDAR DEM to 5-m pixel size. Plan and profile curvatures were then calculated with a square neighborhood size ranging from 15 to 1005 m, which corresponds to a moving window ranging from  $3 \times 3$  to  $201 \times 201$ , respectively.

In *Elevation profiler*, we set the number of circle points to 4000 in order to reduce inaccuracy to less than  $0.1^\circ$ , and we produced elevation profiles for circle diameters ranging from 10 to 1000 m by steps of 10 m (i.e., 100 different profile lengths). The number of SegmPts was set so as to maintain a constant horizontal distance of 1 m between adjacent segment points (e.g., 101 SegmPts for a 100-m long profile segment). Considering the two profile types (transverse and longitudinal) and the 100 different profile lengths, the tool produced a total of 814,000 elevation profiles stored in 1200 tabular data files requiring around 3.4 GB and a few days of computing time on a typical personal computer (e.g., 4 GB DDR3 RAM, Intel® Core i5-650 3.20 GHz).

#### 4.3. Statistical analysis

Differences between CPS and RP in terms of the curvature index ( $\kappa$ ) and the mean curvature profiles were assessed using the Wilcoxon signed rank test for all combinations of study areas, segment lengths (10–1000 m), and profile types (TEP and LEP). When presenting *P*-values (see Figures 4, 5, 7, and B.3 to B.6), we used the usual asterisk rating system based on the following four categories (Motulsky 2013): ‘n.s.’ when  $P > 0.05$  (i.e., statistically not significant), ‘\*’ for  $P < 0.05$  (significant), ‘\*\*’ for  $P < 0.01$  (highly significant), and ‘\*\*\*’ for  $P < 0.001$  (very highly significant). The area between the curves, expressed in per mil of the square of the segment length, was also retained as an alternative method to evaluate the difference between the mean curvature of CPS and RP (see right *y*-axis in Figure 6).

## 5. Results

### 5.1. Curvature $\kappa$ values

Table 3 summarizes the obtained results for the conventional methods ArcMap, ArcSIE, and Landserf, as well as for the proposed approach based on our *Elevation profiler* and *Curvature visualizer*. Remarkable differences were found in terms of sign, magnitude, and degree of dispersion of the  $\kappa$  values, but in general all methods recognize CPS as being slightly more concave (we mean always concave upward) than RP, both in terms of transverse and profile curvature, except in the Arbedo study area where CPS appear to be slightly less concave than RP in the slope direction. In Arbedo and Morobbia, the standard deviation of curvature  $\kappa$  values is generally lower for CPS than for RP, but in Muggio quite the reverse is the case.

The trends of  $\kappa$  values for CPS and RP, with neighborhood size ranging from 10 to 1000 m calculated with the four geomorphometric methods, are presented in Figure 4 for transverse curvature and in Figure 5 for profile curvature. These trends differ considerably, depending on the method of calculation used. However, *P*-values resulting from the



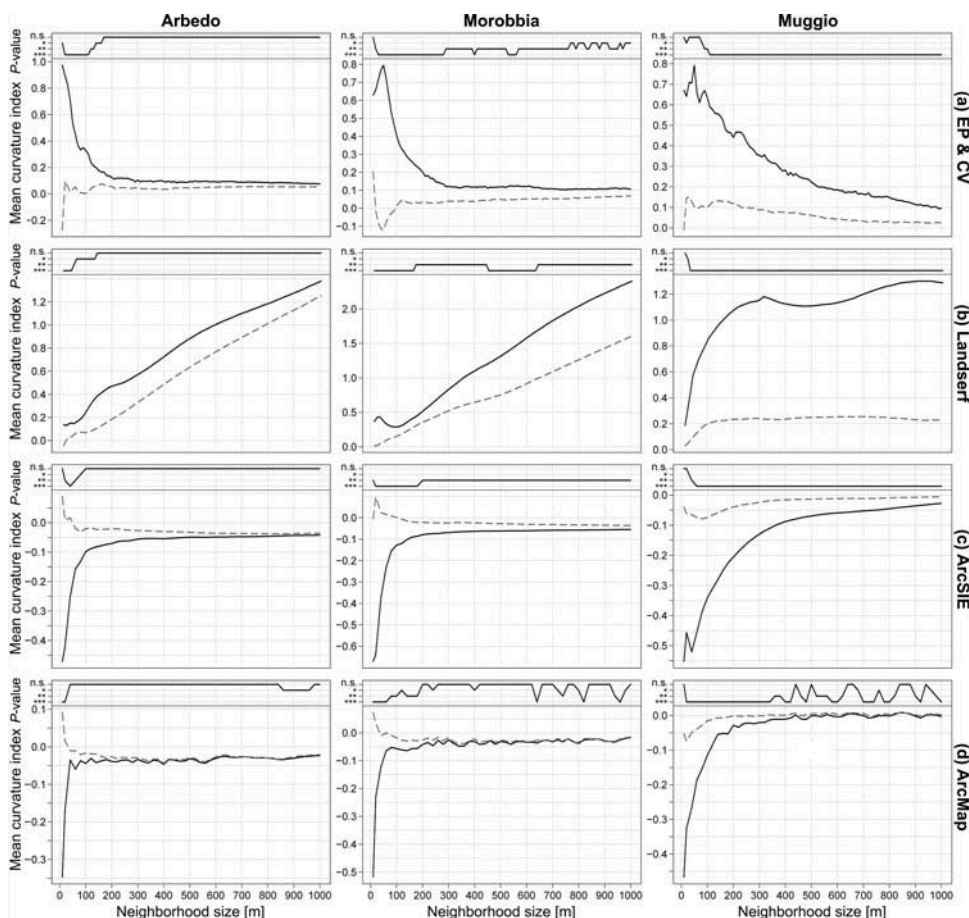


Figure 4. The mean plan curvature (or vertical transverse curvature) of CPS (solid black line) and random points (dashed gray line) in the three study areas, calculated with the four tested geomorphometric methods – (a) *Elevation profiler* and *Curvature visualizer*, (b) *Landserf*, (c) *ArcSIE*, and (d) *ArcMap* – for neighborhood sizes ranging from 10 to 1000 m. In the case of *Landserf* (b), neighborhood sizes range from 15 to 1005 m, while with the new approach (a) neighborhood size coincides with the segment length of transverse elevation profiles (TEP).

Wilcoxon significance tests provide similar estimations of the difference between CPS and RP curvatures for all methods.

All methods reveal to some degree that CPS are not randomly distributed in terms of transverse and profile terrain curvature. Mean  $\kappa$  values of CPS differ statistically from mean  $\kappa$  values of RP (which represent the average terrain curvature of the study areas) both parallel and perpendicular to the line of maximum gradient. These differences are highly significant in Muggio and significant in Morobbia for all neighborhood sizes (i.e., segment lengths, see [Figures 4 and 5](#)). In the Arbedo study area, the differences are significant only for transverse curvature and at small neighborhood sizes (from 10 to 100 m, [Figures 4 and 5](#)). The selectivity of CPS in terms of  $\kappa$  values depends to some degree on the geographical characteristics of the study area, and also from the spatial resolution used as the basis to calculate terrain curvature (i.e., the segment length).



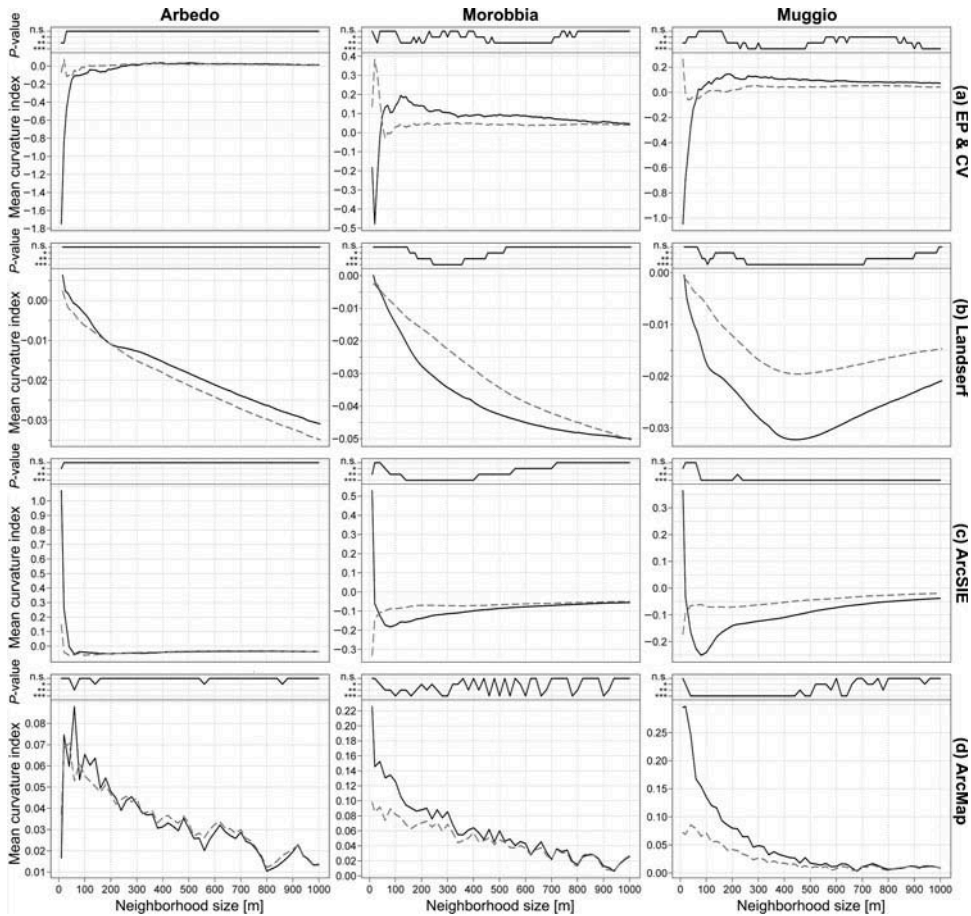


Figure 5. The mean profile curvature (or vertical longitudinal curvature) of CPS (solid black line) and random points (dashed gray line) in the three study areas, calculated with the four tested geomorphometric methods – (a) *Elevation profiler* and *Curvature visualizer*, (b) *Landserf*, (c) *ArcSIE*, (d) *ArcMap* – for neighborhood sizes ranging from 10 to 1000 m. In the case of *Landserf* (b), neighborhood sizes range from 15 to 1005 m, while with the new approach (a) neighborhood size coincides with the segment length of longitudinal elevation profiles (LEP).

## 5.2. Transverse profile curvatures

Figure 7a shows the half transverse elevation profiles (half-TEP) for a fixed segment length of 230 m, which is a graphical representation of the shape of the terrain surface in the transverse direction related to the absolute horizontal distance from the site, obtained by averaging the two semi-axes of every TEP. The half-TEP mean curvature reveals a slightly concave profile for both the CPS and the RP in all three study areas. In other words, if we move away from a site along an axis perpendicular to the slope, on average, the terrain surface tends to rise regardless of which of the two semi-axes we follow. Despite this global trend, the CPS can be clearly distinguished from random points since the gradient of their average half-TEP profile is much more marked. When expressed in degrees, the maximum difference between CPS and RP is found in Arbedo, at a segment length of 300 m (CPS 2.5°, RP 1.0°,  $\Delta$  1.5°), in Morobbia at a segment length of 790 m

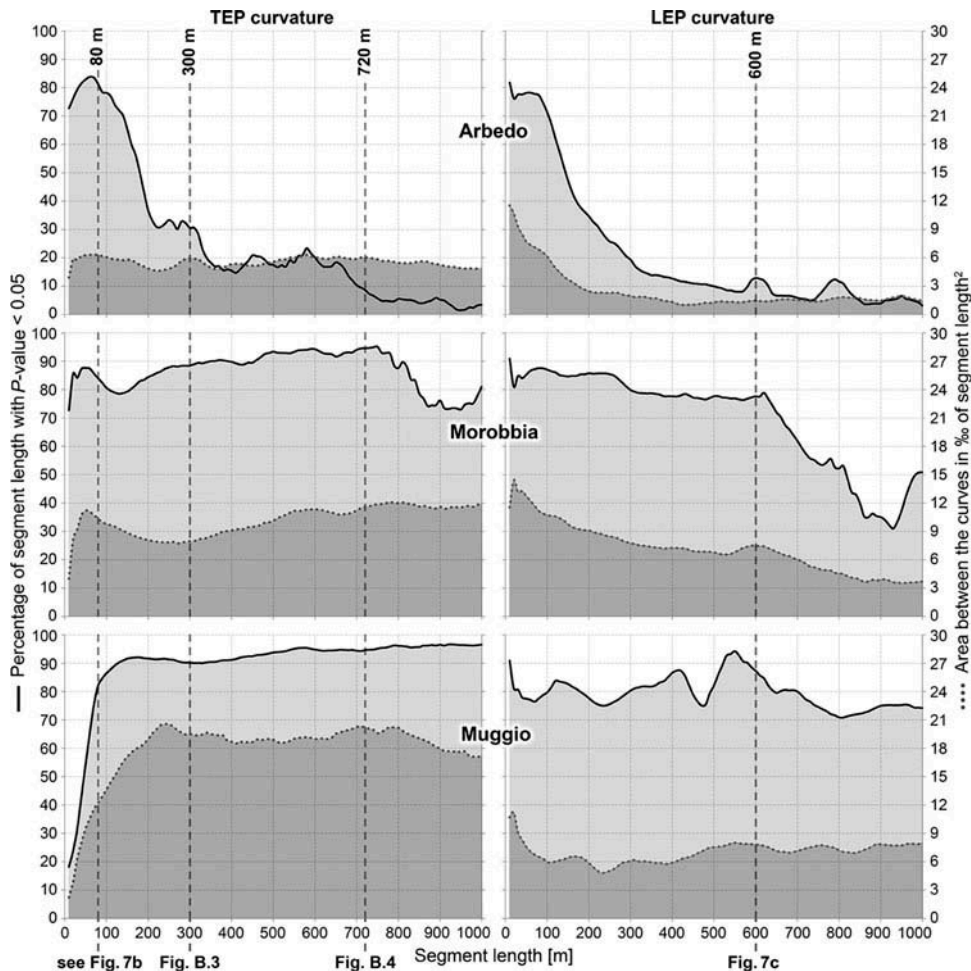


Figure 6. The difference between CPS and random points in the three study areas in terms of average TEP and LEP curvature according to profile segment length. The difference is expressed as percentage of the segment length with significant  $P$ -values (solid black line) and as area between the curves in per mil of the square of the segment length (dashed gray line). The vertical dotted gray lines highlight the segment lengths that were chosen for a more in-depth analysis of the data, that is, 80, 300, and 720 m for the TEP curvature (see Figures 7b, B.3, and B.4) and 600 m for the LEP curvature (see Figure 7c).

(CPS  $6.3^\circ$ , RP  $3.3^\circ$ ,  $\Delta$   $3.0^\circ$ ), and in Muggio at a segment length of 230 m (CPS  $5.9^\circ$ , RP  $0.9^\circ$ ,  $\Delta$   $5.0^\circ$ ). Considering the segment length of up to 1000 m, the mean differences between CPS and RP are  $1.2^\circ$  in Arbedo,  $2.2^\circ$  in Morobbia, and  $3.7^\circ$  in Muggio (data not shown). The difference between the two curves of the half-TEP mean curvature for the CPS and RP is highly significant in Muggio for all segment lengths, and significant in Morobbia for a large range of segment lengths, ranging from 10 m to approximately 2.5 km (data not shown). In the case of Arbedo, the difference is significant only for segment lengths ranging from 10 to 170 m (data not shown).

Figure 7b shows the full-TEP mean curvatures for a segment length of 80 m calculated by averaging the complete TEP, turned so as to have the semi-axis with the higher sum in

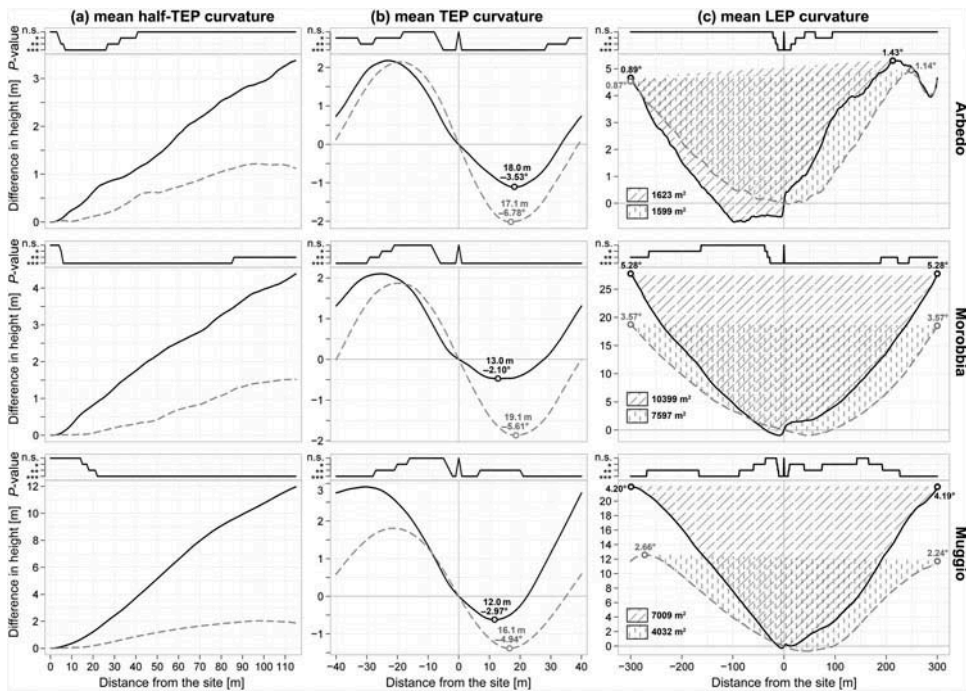


Figure 7. The mean transverse (a and b) and longitudinal (c) profiles of curvature of CPS (solid black line) and random points (dashed gray line) in the three study areas. The significance of the difference between CPS and RP, according to the Wilcoxon signed rank test, is presented by plotting the usual four categories of  $P$ -values in the upper part of each graph. The mean half-TEP curvature (a) is based on a segment length of 230 m. By averaging the two semi-axes of each TEP, the half-TEP graph shows the vertical displacement of the terrain surface in relation to the absolute horizontal distance from the site, regardless of the direction of the departure from the center of the segment. The mean TEP curvature (b) is based on a segment length of 80 m. For this averaging, all elevation profiles were rotated in order to have the half of the profile segment with the higher sum always on the left side of the  $x$ -axis. On each curve, we marked the minimum point (i.e., the trough) with a small circle (black for CPS and gray for RP), and we indicated its distance and angle with respect to the zero point (i.e., the origin). The mean LEP curvature (c) is based on a segment length of 600 m. The upward half of the LEP is always on the left side of the  $x$ -axis. The area of the concavity for CPS and RP is presented numerically (in square meters) and graphically (by the means of two grid patterns). On the upper and lower side of each mean profile, we marked the maximum point with a small circle (black for CPS and gray for RP), and we indicated its angle with respect to the zero point (i.e., the origin).

terms of  $y$ -values on the left (see also B.3 to B.5 for other segment lengths). As reported in Figure 6, in Muggio differences in full-TEP mean curvature between CPS and RP are highly significant for all segment lengths, in Morobbia for most segment lengths, while in Arbedo the differences are significant only for shorter segments.

The position of random points, represented by the zero point on the graph of the full-TEP mean curvature (Figure 7b and B.3 to B.5), is near the middle, between the upper and the lower point of the sinusoid, with only a slight shift toward the trough. For CPS, this shift is much greater, and the sites tend to be closer to the lowest point of the profile and more distant from the highest point of the profile. For instance, in the range of segment lengths from 10 to 1000 m, the oblique line connecting the zero point to the trough has, on

Table 3. Comparison among the mean plan (or transverse) and profile  $\kappa$  values obtained with the four tested geomorphometric methods (ArcMap, ArcSIE, Landserf, and *Elevation profiler* and *Curvature visualizer*) in the three study areas for CPS and RP.

Study area	Category of sites	Neighborhood size [m]	Mean curvature index							
			Plan (or transverse)			Profile				
			ArcMap	ArcSIE	Landserf	EP & CV	ArcMap	ArcSIE	Landserf	EP & CV
Arbedo	CPS	60	-0.060 ± 0.453	-0.158 ± 1.279	0.162 ± 1.378	0.451 ± 3.076	0.088 ± 0.340	-0.056 ± 0.808	-0.001 ± 0.041	-0.108 ± 1.556
		200	-0.039 ± 0.131	-0.071 ± 0.435	0.474 ± 2.203	0.122 ± 1.077	0.048 ± 0.090	-0.053 ± 0.265	-0.011 ± 0.044	-0.039 ± 0.581
		800	-0.030 ± 0.029	-0.046 ± 0.102	1.187 ± 2.403	0.087 ± 0.296	0.010 ± 0.022	-0.035 ± 0.058	-0.026 ± 0.046	0.024 ± 0.140
		All	-0.043 ± 0.157	-0.077 ± 0.437	0.833 ± 2.182	0.149 ± 0.857	0.033 ± 0.121	-0.012 ± 0.336	-0.018 ± 0.042	-0.030 ± 0.532
		60	-0.011 ± 0.431	-0.019 ± 1.460	0.067 ± 1.381	0.053 ± 3.157	0.053 ± 0.361	-0.059 ± 1.036	-0.004 ± 0.049	-0.045 ± 2.060
Morobbia	CPS	200	-0.026 ± 0.140	-0.022 ± 0.416	0.191 ± 1.694	0.054 ± 1.097	0.047 ± 0.093	-0.051 ± 0.291	-0.011 ± 0.046	0.008 ± 0.632
		800	-0.030 ± 0.031	-0.038 ± 0.108	1.016 ± 2.501	0.053 ± 0.282	0.012 ± 0.024	-0.037 ± 0.067	-0.030 ± 0.051	0.014 ± 0.149
		All	-0.025 ± 0.171	-0.027 ± 0.502	0.625 ± 2.092	0.044 ± 0.925	0.034 ± 0.141	-0.039 ± 0.492	-0.021 ± 0.048	0.010 ± 0.624
		60	-0.065 ± 0.319	-0.232 ± 0.930	0.322 ± 1.086	0.723 ± 2.220	0.131 ± 0.314	-0.173 ± 0.765	-0.009 ± 0.043	0.133 ± 1.651
		200	-0.042 ± 0.136	-0.079 ± 0.300	0.529 ± 1.740	0.201 ± 0.789	0.088 ± 0.116	-0.138 ± 0.271	-0.028 ± 0.057	0.141 ± 0.617
Muggio	RP	800	-0.038 ± 0.030	-0.058 ± 0.117	2.047 ± 3.431	0.106 ± 0.275	0.015 ± 0.012	-0.064 ± 0.078	-0.048 ± 0.057	0.063 ± 0.175
		All	-0.051 ± 0.131	-0.101 ± 0.341	1.332 ± 2.666	0.185 ± 0.673	0.061 ± 0.115	-0.083 ± 0.309	-0.038 ± 0.056	0.078 ± 0.548
		60	-0.001 ± 0.419	0.016 ± 1.243	0.103 ± 1.411	-0.078 ± 2.662	0.074 ± 0.322	-0.098 ± 0.902	-0.007 ± 0.046	-0.030 ± 2.165
		200	-0.027 ± 0.143	-0.021 ± 0.384	0.364 ± 1.897	0.035 ± 1.028	0.071 ± 0.117	-0.070 ± 0.276	-0.016 ± 0.049	0.041 ± 0.700
		800	-0.035 ± 0.030	-0.034 ± 0.110	1.267 ± 3.009	0.055 ± 0.271	0.013 ± 0.014	-0.056 ± 0.081	-0.045 ± 0.058	0.044 ± 0.174
Muggio	CPS	All	-0.023 ± 0.159	-0.022 ± 0.425	0.807 ± 2.466	0.041 ± 0.846	0.046 ± 0.128	-0.073 ± 0.389	-0.032 ± 0.055	0.049 ± 0.650
		60	-0.186 ± 0.538	-0.455 ± 1.534	0.688 ± 2.126	0.659 ± 3.495	0.168 ± 0.365	-0.226 ± 0.937	-0.011 ± 0.046	-0.065 ± 1.491
		200	-0.028 ± 0.130	-0.206 ± 0.517	1.082 ± 2.738	0.440 ± 1.287	0.080 ± 0.123	-0.140 ± 0.303	-0.023 ± 0.052	0.135 ± 0.622
		800	-0.002 ± 0.021	-0.045 ± 0.106	1.265 ± 3.408	0.148 ± 0.329	0.006 ± 0.020	-0.050 ± 0.075	-0.025 ± 0.048	0.079 ± 0.184
		All	-0.039 ± 0.165	-0.134 ± 0.458	1.110 ± 2.985	0.293 ± 0.974	0.052 ± 0.130	-0.089 ± 0.315	-0.025 ± 0.049	0.061 ± 0.551
Muggio	RP	60	-0.039 ± 0.523	-0.074 ± 1.196	0.139 ± 1.577	0.092 ± 2.447	0.079 ± 0.320	-0.064 ± 0.699	-0.004 ± 0.038	-0.030 ± 1.174
		200	-0.001 ± 0.138	-0.040 ± 0.493	0.235 ± 2.367	0.119 ± 1.119	0.042 ± 0.100	-0.071 ± 0.247	-0.012 ± 0.043	0.019 ± 0.420
		800	0.004 ± 0.020	-0.009 ± 0.093	0.243 ± 2.503	0.032 ± 0.323	0.004 ± 0.019	-0.026 ± 0.067	-0.016 ± 0.041	0.053 ± 0.173
		All	-0.004 ± 0.146	-0.024 ± 0.388	0.228 ± 2.345	0.064 ± 0.855	0.024 ± 0.102	-0.048 ± 0.257	-0.015 ± 0.042	0.037 ± 0.447

Note: We present a selection of results related to three neighborhood sizes (60, 200, and 800 m), as well as the grand mean taking into account the entire range of neighborhood sizes from 10 to 1000 m. Each mean curvature index is accompanied by its standard deviation. The signs adopted for concavity are indicated below the method.

average, greater negative inclinations for the RP ( $-6.5^\circ$  for Arbedo,  $-5.7^\circ$  for Morobbia, and  $-6.9^\circ$  for Muggio) than for the CPS ( $-5.5^\circ$ ,  $-4.0^\circ$ , and  $-4.5^\circ$ , respectively), and is much shorter for CPS than for RP with reductions in length of 0.65 for Muggio, 0.76 for Morobbia, and only 0.96 for Arbedo (data not shown).

### 5.3. Longitudinal profile curvatures

The visualization of the longitudinal curvature around RP reveals a slight concavity in all study areas. In the case of a 600-m-long LEP (Figure 7c), moving away from the center toward the maximum points, the line representing the average curvature goes up with a mean angle of  $2.66^\circ$  upwardly and  $2.24^\circ$  downwardly in Muggio. In Morobbia, this angle is even more pronounced ( $3.57^\circ$ ), while in Arbedo it is almost negligible ( $0.87^\circ$  upwardly and  $1.14^\circ$  downwardly). Also, the longitudinal curvature around CPS is concave, but with a more marked depression and a clearer and more sudden break of slope, with a reduction in the gradient coinciding with the center of the segment. Moving away from the center toward the maximum points, the mean angle is around  $4.2^\circ$  in Muggio and  $5.3^\circ$  in Morobbia, while in Arbedo this angle is lower upwardly ( $0.89^\circ$ ) than downwardly ( $1.43^\circ$ ). For Muggio and Morobbia, the differences between CPS and RP are significant over a wide range of segment lengths (Figures 6 and 7c), while in Arbedo, they are significant only for the shorter segments (Figure B.6).

## 6. Discussion

### 6.1. The limits of curvature index

With the advent of geomorphometry, many methods were conceived that are well suited to the task of quickly assigning a curvature index to every cell of a raster layer. Once stored in a georeferenced grid, the curvature data can be easily used for all sorts of GIS analysis. The question whether these cellular indices are always the best way to represent, describe, and analyze the curvature of the terrain surface remains open, however. The analysis of terrain curvature around CPS is a good test case to check the limits of the different methods. The most common procedure included in several commercial and open-source GIS software packages calculates the curvatures for each cell of the DEM raster data set solely using its eight immediate neighbors. The only way for the user to get larger neighborhoods is to first resample the DEM changing its cell size. Our test case shows that this method, implemented in ArcMap, tends to produce uneven results starting from neighborhood sizes of 200–360 m in Morobbia and 440–600 m in Muggio, and does not permit the clear evaluation of the differences between CPS and RP in terms of transverse and profile curvature (Figures 4d and 5d). Such a decrease in reliability for larger neighborhoods is certainly due to the initial resampling of the DEM and the consequent depletion of elevation data. Beyond a certain limit of DEM simplification, the resulting terrain morphometric attributes tend to become inaccurate.

In this sense, the other two conventional methods applied in our test case (ArcSIE and Landserf) proved to be more robust and effective in assessing transverse and profile curvature even at large spatial scales (Figures 4b, 4c, 5b, and 5c) thanks to the possibility of selecting the neighborhood size independently of the DEM cell resolution.

With these advanced methods, it is possible to precisely calculate the average curvature over large terrain surfaces, without the need to resample and simplify the input DEM. There are, however, a number of drawbacks. The first is the calculation time. In Landserf,



computation times tend to become very long (i.e., many minutes or even many hours) when handling DEM with more than one million points (e.g.,  $>1000 \times 1000$  elevation data) and when setting neighborhood windows with more than 1000 values (i.e.,  $>31 \times 31$  pixels). Difficult to understand is the fact that the absolute  $\kappa$  values computed with Landserf are generally the highest for the plan curvature and the lowest for the profile curvature compared to those calculated with the other methods (Table 3, Figures 4b and 5b). Secondly, the method-dependent differences in terms of units, sign, amplitude, statistical dispersion, and pattern make curvature measurements difficult to interpret and compare. As pointed out by one of the pioneers of modern geomorphometry, the ‘numerous variant definitions of curvature have complicated matters, reducing the simplification originally desired’ (Evans 2013). In fact, the diversification of methods and techniques has somewhat dampened the initial enthusiasm of those who considered the system of the five fundamental attributes (altitude, gradient, aspect, plan, and profile convexity) as the main pillar of geomorphometry (Evans 1972, 1980, Krcho 1973, Goudie et al. 2005).

Finally, conventional methods do not offer any kind of graphical visualization to complement the indices of curvature that would facilitate their interpretation. As stated by Wood (2009b), it is regrettable that geomorphometry does not really take advantage of recent development in visualization. In fact,  $\kappa$  values are not self-evident and their interpretation can be tricky, especially without any additional information allowing the user to visually evaluate the relationship between the shape of the ground and the resulting  $\kappa$  value. Terrain curvature is a continuous and multiscale surface attribute and, consequently, a matrix of  $\kappa$  values cannot provide a comprehensive representation of reality.

## 6.2. The novel approach to calculate and visualize the index of curvature

By using, in sequence, the VBA macro *Elevation profiler* to build TEP and longitudinal elevation profile (LEP) for all CPS and RP, and the *Curvature visualizer* R script to calculate the  $\kappa$  values, we obtained a summary of the trends of the mean transverse and profile curvature index for CPS and RP in the three study areas and for a range of neighborhood sizes going from 10 to 1000 m (Figures 4a and 5a). By comparing this summary with those obtained with Landserf (Figures 4b and 5b) and ArcSIE (Figures 4c and 5c), and by correctly interpreting the sign and the amplitude of  $\kappa$  values, we can conclude that the various methods provide quite similar results. This is encouraging since it shows that our method, while using a very specific procedure, provides reliable results that do not differ much from the outputs of conventional methods.

In contrast to classical methods, our approach offers to users the ability to set the degree of the polynomial function that will be used to approximate the elevation profiles and to assess, in various ways, the quality of fit, which is a crucial step in the calculation of the index of curvature. Starting from the output table summarizing the coefficient of determination ( $R^2$ ), the user can, for example, easily display the goodness of fit in the form of a scatter plot. In our test case, by approximating the TEP and LEP of CPS with sixth-degree polynomials, the median of the goodness of fit remains nearly always above 90% in every study area and for every profile segment length (Figures B.1 and B.2). In this regard, Landserf, for instance, permits neither the choice of the complexity of the function used to fit the elevation data, nor the evaluation of the goodness of fit of the polynomial surface in representing the elevation model in the selected window size. Another advantage of our approach is the possibility to visualize the TEP and LEP of individual sites, complete with all relevant numerical and graphical information concerning the curvature ( $\kappa$  value,  $R^2$ , polynomial function, and osculating circle). The *Curvature*



*visualizer* assembles and outputs these curvature profiles for all sites in a practical pdf file (see, for instance, the file ‘Muggio\_CPS\_TEP\_300m.pdf’ in the supplementary electronic materials that reports the TEP of 300 m in length for all 347 CPS inventoried in the Muggio study area). Please note that with the *Curvature visualizer*, the user can choose to force the polynomial function (depicted by the solid purple line in the profiles) to pass through the origin, that is, through the point representing the specific study site. In addition, the user may also choose the aspect ratio relating the *x*-axis to the *y*-axis of the plots. When the scale of the two axes is set as independent, the script automatically selects the more suitable scale for the *y*-axis, producing a vertical exaggeration and forcing the osculating circles to be drawn as ellipses (depicted by the red dashed lines in the profiles).

### 6.3. The average curvature profile

An additional interesting feature provided by the new approach is the possibility of calculating the mean TEP or LEP curvature by averaging all profile data. This makes it possible to obtain an effective representation of the curvature of the terrain around a specific category of sites. These average profiles of curvature have never been considered and exploited as a mean of analysis in geomorphometry. We are convinced that this type of Cartesian representation of the average curvature has great potential in terms of amount of information conveyed, simplicity and ease of understanding, and new analytical possibilities. Compared to a mean  $\kappa$  value, an average curvature profile provides a more comprehensive description of the curvature of a particular category of sites, and, in addition, it is easier to understand and interpret. In short, it enables the graphical representation of the shape and spatial dimension of the curvature, and offers several operational and performance advantages that we can summarize as follows:

- The curvature profiles are very similar to common elevation profiles, and, as such, they are easily readable and understandable because they represent the shape of the depicted surface.
- Unlike the difficulties of interpretation related to the sign of the curvature index, in the case of curvature profiles the distinction between concavity and convexity can be easily made by considering the shape of the profile.
- The profile provides a continuous representation of the curvature by using real quantities and common metric units of measurements. In our TEP and LEP profiles, we applied a vertical exaggeration (usually between  $\times 10$  and  $\times 20$ ) to emphasize vertical features and consequently highlight the curvature (Figures 7 and B.3 to B.6). One can, however, also use the same scale for the two axes and thus obtain a more realistic representation of the curvilinear form of terrain surface (Figure A.6).
- Starting from the TEP and LEP profiles, one can easily carry out many different measurements (e.g., horizontal and vertical distances from the crest and the trough, mean angles, area of the concavity, energy consumption) to better describe and analyze the characteristics of the curvature.
- It is possible to calculate the significance of the difference between mean curvature profiles ascertaining whether different categories of sites have different curvature patterns.

The drawbacks of this alternative method of calculation and analysis of the land surface curvature are the following:

- A more time-consuming calculation with respect to the well-established methods of curvature computation, especially when working with long profile segments and high levels of spatial resolution.
- The higher amount of storage space occupied by the resulting tabular data files in comparison to common curvature grids.
- The need to process these files with R scripts in order to obtain any kind of information such as graphic charts, statistical analyses, or topographic measurements.
- The lack of the possibility of calculating the global curvature in addition to the transverse and longitudinal curvature.

Figure 7c is a good example of the amount of information on curvature that a mean LEP can provides. The longitudinal profiles for the three study areas are computed here for a segment length of 600 m, which is over a quite large spatial scale. On this scale, the mean  $\kappa$  values show only slight differences between RP and CPS that are difficult to interpret (Figure 5). For instance, using ArcSIE, we obtain the following mean values (Figure 5c):  $-0.039$  for RP and  $-0.036$  for CPS in Arbedo;  $-0.062$  for RP and  $-0.077$  for CPS in Morobbia; and  $-0.038$  for RP and  $-0.073$  for CPS in Muggio. The negative sign indicates that both RP and CPS are slightly concave, and that CPS are a little bit more concave than RP at least in Morobbia and Muggio. But differences are so minimal that they may also result from the fact that charcoal sites are anthropogenically modified with concavity artificially created at the upper side and convexity at the downslope side (Figure 2). Thanks to the mean LEP (Figure 7c), we obtain instead a detailed visualization of these differences. In particular, the geomorphic effect of the platforms artificially created by charcoal burners is clearly visible at the origin of the profiles ( $x, y = 0$ ). In Arbedo, this effect is particularly marked with an impact over large part of the profile. Instead, in Morobbia and Muggio, this effect is limited to the close proximity of CPS, while the concavity at broader scale and the location of CPS at the break of slope are related to the way CPS were selected. In addition, mean LEP offers the possibility to express the curvature in terms of area of the concavity/convexity. In the case of 600 m long longitudinal profiles (Figure 7c), the maximal concavity is observed for CPS in Morobbia ( $10392 \text{ m}^2$ ), while the higher difference between RP and CPS is observed in Muggio with an areal ratio of approximately 1:1.74 ( $4032$  against  $7009 \text{ m}^2$ ).

## 7. Conclusion

Terrain curvature is a key morphometric variable that has a great variety and number of applications. Despite its importance, conventional calculation methodology has remained practically unchanged over the past decades. On the one hand, these methods enhance the complexity because they use a polynomial three-dimensional surface to approximate the elevation data, even when calculating transverse and profile curvature that are the attributes of two-dimensional curves. On the other hand, they are prone to oversimplification because they reduce the irregular, multiscalar, and curvilinear forms of land surface to single  $\kappa$  values, or grids of numbers, which may be not informative enough for studying the topography of selected sites.

In this study, we attempted to overcome these limitations by developing new GIS tools to represent graphically and measure the shape and spatial dimensions of curvature. Our approach proved to be reliable even for very large neighborhood sizes, providing quite

similar results in terms of mean  $\kappa$  values for CPS and RP with respect to the well-established reference methods. One of the advantages of our approach is the full control on curve fitting through the choice of degree of the polynomial function, the visualization of the fitted curve on elevation profiles, and the report of the goodness of fit. Moreover, the tool permits visualization of the convexity of terrain through curvature profiles, thus avoiding the inherent oversimplification of  $\kappa$  values.

The shift from a single-point value to a curvature profile is a decisive step opening new possibilities. For instance, half transverse profiles show terrain curvature in a very clear and simple way, with a significant increase of quantitative information, compared to the common indices of curvature. On the other hand, full transverse profiles offer the advantage of accounting also for the differences between the two semi-axes of the elevation profile. Thanks to the initial ordering of the profiles, the graph of the full-TEP mean curvature tends to become a wavy line (i.e., a single cycle of a sinusoid) that clearly shows the average and relative position of the sites with respect to the main neighboring concave and convex forms or, specifically in our test case, to the mountain stream channels (represented by the crest of the sine wave) and ridges (represented by the trough of the sine wave), respectively.

The new method makes it possible to visualize, characterize, and compare the convexity around different types of sites, thus offering the means and motivation to pay greater attention to land surface curvature. Last but not the least, the *Elevation profiler* enables the automatic calculation of TEP and LEP, starting from a DEM and a point shapefile, which could be useful in many different fields.

We are aware that such a complex approach is particularly suitable for cases where curvature is a prominent part of the object of study. When curvature is just a morphological parameter among many others, it is often preferable to apply routine quantifications so as to reduce the complexity of terrain curvature to a single value per surface unit.

In our test case, the curvature profiles turned out to be a good way to demonstrate that charcoal burners paid some attention to land surface curvature when choosing and preparing places for carbonization. Convex sites were generally avoided. As a result, CPS tend to occupy more concave places, both in terms of TEP and LEP curvature, and on both small and large spatial scales. On average, CPS are closer to the bottom of runoff channels and more distant from the top of ridges, without being coincident with the axis of the concave features. These results suggest further research, especially in the field of historical geography, to answer remaining questions concerning the location of CPS. In this respect, it would be useful to review the existing historical and ethnographic documentation in order to obtain a summary of what has been written on the qualities required for CPS.

### Acknowledgements

Our heartfelt thanks go to Matteo Minetti, Philippe Wäger, Joël Godat, Matthias von Rohr, Luca Pampuri, and Ferdinand Hermann for the field work, to Curtis Gautschi for the English revision of the manuscript, and to the reviewers for the remarks that helped us to improve the text.

### Supplementary material

Supplementary material (i.e., Appendix A with Figures A.1, A.2, A.3, A.4, A.5, and A.6; Appendix B with Figures B.1, B.2, B.3, B.4, B.5, and B.6; files *ElevationProfiler\_ScreenShots.zip* and

Muggio\_CPS\_TEP\_300m.pdf) for this article can be accessed <http://dx.doi.org/10.1080/13658816.2014.995102>.

## References

- Abate, M. and Tavena, F., 2012. *Curves and surfaces*. New York, NY: Springer.
- Albani, M. and Klinkenberg, B., 2003. A spatial filter for the removal of striping artifacts in digital elevation models. *Photogrammetric Engineering and Remote Sensing*, 69 (7), 755–765. doi:10.14358/PERS.69.7.755
- Albani, M., et al., 2004. The choice of window size in approximating topographic surfaces from digital elevation models. *International Journal of Geographical Information Science*, 18 (6), 577–593. doi:10.1080/13658810410001701987
- Blaga, L., 2012. Aspects regarding the significance of the curvature types and values in the studies of geomorphometry assisted by GIS. *Analele Universității din Oradea – Seria Geografie*, 22 (2), 327–337.
- Corripio, J.G., 2003. Vectorial algebra algorithms for calculating terrain parameters from DEMs and solar radiation modelling in mountainous terrain. *International Journal of Geographical Information Science*, 17 (1), 1–23. doi:10.1080/713811744
- Curtis, L.F., Doornkamp, J.C., and Gregory, K.J., 1965. The description of relief in field studies of soils. *Journal of Soil Science*, 16 (1), 16–30. doi:10.1111/j.1365-2389.1965.tb01417.x
- De Smith, M.J., Goodchild, M.F., and Longley, P., 2007. *Geospatial analysis: a comprehensive guide to principles, techniques and software tools*. Leicester: Matador.
- Dong, Y., Tang, G., and Zhang, T., 2008. A systematic classification research of topographic descriptive attribute in digital terrain analysis. *The International Archives of the Photogrammetry, Remote Sensing and Spatial Information Sciences*, 37 (B2), 357–362.
- Erskine, R.H., et al., 2007. Digital elevation accuracy and grid cell size: effects on estimated terrain attributes. *Soil Science Society of America Journal*, 71 (4), 1371–1380. doi:10.2136/sssaj2005.0142
- Evans, I.S., 1972. General geomorphology, derivatives of altitude and descriptive statistics. In: R.J. Chorley, ed. *Spatial analysis in geomorphology*. London: Methuen, 17–90.
- Evans, I.S., 1979. *Statistical characterization of altitude matrices by computer. An integrated system of terrain analysis and slope mapping*. Durham: Department of Geography, University of Durham.
- Evans, I.S., 1980. An integrated system of terrain analysis and slope mapping. *Zeitschrift für Geomorphologie*, 36, 274–295.
- Evans, I.S., 2013. Land surface derivatives: history, calculation and further development. In: *Proceedings of geomorphometry*, 16–20 October 2013, Nanjing, China.
- Florinsky, I.V., 1998. Accuracy of local topographic variables derived from digital elevation models. *International Journal of Geographical Information Science*, 12 (1), 47–62. doi:10.1080/136588198242003
- Florinsky, I.V., 2011. *Digital terrain analysis in soil science and geology*. Amsterdam: Academic Press.
- Florinsky, I.V. and Kuryakova, G.A., 1996. Influence of topography on some vegetation cover properties. *Catena*, 27 (2), 123–141. doi:10.1016/0341-8162(96)00005-7
- Gao, J., Burt, J.E., and Zhu, A.-X., 2012. Neighborhood size and spatial scale in raster-based slope calculations. *International Journal of Geographical Information Science*, 26 (10), 1959–1978. doi:10.1080/13658816.2012.657201
- Goudie, A., et al., 2005. *Geomorphological techniques*. London: Routledge.
- Hart, B.S. and Sagan, J.A., 2007. Curvature for visualization of seismic geomorphology. In: R.J. Davies, ed. *Seismic geomorphology: applications to hydrocarbon exploration and production*. London: Geological Society, 139–149.
- Hengl, T. and Reuter, H.I., 2009. *Geomorphometry: concepts, software, applications*. Amsterdam: Elsevier.
- Huggett, R.J. and Cheeseman, J., 2002. *Topography and the environment*. Harlow: Pearson Education.
- Hurst, M.D., et al., 2012. Using hilltop curvature to derive the spatial distribution of erosion rates. *Journal of Geophysical Research*, 117, F02017. doi:10.1029/2011JF002057
- Jenness, J., 2013. *DEM surface tools for ArcGIS*. Flagstaff, AZ: Jenness Enterprises.

- Knoebel, A., *et al.*, 2007. *Mathematical masterpieces. Further chronicles by the explorers*. New York: Springer.
- Krcho, J., 1973. Morphometric analysis of relief on the basis of geometric aspect of field theory. *Acta geographica Universitatis Comenianae. Seria Geographico-physica*, 1, 7–233.
- Ludemann, T., Michiels, H.-G., and Nölken, W., 2004. Spatial patterns of past wood exploitation, natural wood supply and growth conditions: indications of natural tree species distribution by anthracological studies of charcoal-burning remains. *European Journal of Forest Research*, 123 (4), 283–292. doi:10.1007/s10342-004-0049-z
- Milevski, I., 2007. Morphometric elements of terrain morphology in the Republic of Macedonia and their influence on soil erosion. In: *International conference "Erosion and torrent control as a factor in sustainable river basin management"*, 25–28 September 2007, Belgrade, Serbia.
- Minár, J., *et al.*, 2013. Third-order geomorphometric variables (derivatives): definition, computation and utilization of changes of curvatures. *International Journal of Geographical Information Science*, 27 (7), 1381–1402. doi:10.1080/13658816.2013.792113
- Moore, I.D., Grayson, R.B., and Ladson, A.R., 1991. Digital terrain modeling: a review of hydrological, geomorphological, and biological applications. *Hydrological Processes*, 5, 3–30. doi:10.1002/hyp.3360050103
- Mortimer, R.G., 2005. *Mathematics for physical chemistry*. Amsterdam: Academic Press.
- Motulsky, H., 2013. *Intuitive biostatistics: a nonmathematical guide to statistical thinking*. Oxford: Oxford University Press.
- O'Callaghan, J.F. and Mark, D.M., 1984. The extraction of drainage networks from digital elevation data. *Computer Vision, Graphics, and Image Processing*, 28 (3), 323–344. doi:10.1016/S0734-189X(84)80011-0
- Peckham, S.D., 2011. Profile, plan and streamline curvature: a simple derivation and applications. In: *Proceedings of Geomorphometry*, 7–11 September 2011, Redlands, CA.
- Peucker, T.K. and Douglas, D.H., 1975. Detection of surface-specific points by local parallel processing of discrete terrain elevation data. *Computer Graphics and Image Processing*, 4, 375–387. doi:10.1016/0146-664X(75)90005-2
- Porres de la Haza, M.J. and Pardo Pascual, J.E., 2002. Comparison between the different curvature models of terrain for determining the degree of soil humidity. In: J.A. Sobrino, ed. *Recent advances in quantitative remote sensing*. Valencia: Universitat de València, 238–245.
- Prasicek, G., *et al.*, 2014. Multi-scale curvature for automated identification of glaciated mountain landscapes. *Geomorphology*, 209, 53–65. doi:10.1016/j.geomorph.2013.11.026
- R Core Team, 2013. *R: a language and environment for statistical computing*. Vienna: R Foundation for Statistical Computing. Available from: <http://www.R-project.org/> [Accessed 10 November 2014].
- Rennie, E.B., 1997. *The recessed platforms of Argyll, Bute and Inverness*. Oxford: Archaeopress.
- Romstad, B. and Etzelmüller, B., 2012. Mean-curvature watersheds: a simple method for segmentation of a digital elevation model into terrain units. *Geomorphology*, 139–140, 293–302. doi:10.1016/j.geomorph.2011.10.031
- Schmidt, J., Evans, I.S., and Brinkmann, J., 2003. Comparison of polynomial models for land surface curvature calculation. *International Journal of Geographical Information Science*, 17 (8), 797–814. doi:10.1080/13658810310001596058
- Shary, P.A., 1995. Land surface in gravity points classification by a complete system of curvatures. *Mathematical Geology*, 27 (3), 373–390. doi:10.1007/BF02084608
- Shary, P.A., 2008. Models of topography. In: Q. Zhou, B. Lees, and G. Tang, eds. *Advances in digital terrain analysis*. Berlin: Springer, 29–57.
- Shary, P.A., Sharaya, L.S., and Mitusov, A.V., 2002. Fundamental quantitative methods of land surface analysis. *Geoderma*, 107, 1–32. doi:10.1016/S0016-7061(01)00136-7
- Shary, P.A., Sharaya, L.S., and Mitusov, A.V., 2005. The problem of scale-specific and scale-free approaches in geomorphometry. *Geografia Fisica e Dinamica Quaternaria*, 28, 81–101.
- Shi, X., 2013. *ArcSIE user's guide*. Bow, NH: Spatial Inference Enterprises.
- Shi, X., *et al.*, 2007. An experiment using a circular neighborhood to calculate slope gradient from a DEM. *Photogrammetric Engineering & Remote Sensing*, 73 (2), 143–154. doi:10.14358/PERS.73.2.143
- Smith, R.B., 2012. *Analyzing terrain and surfaces with TNTmips®*. Lincoln: MicroImages.

- Sofia, G., Pirotti, F., and Tarolli, P., 2013. Variations in multiscale curvature distribution and signatures of LiDAR DTM errors. *Earth Surface Processes and Landforms*, 38 (10), 1116–1134. doi:[10.1002/esp.3363](https://doi.org/10.1002/esp.3363)
- Speight, J.G., 1968. Parametric description of land form. In: G.A. Stewart, ed. *Land evaluation*. Melbourne: Macmillan, 239–250.
- Svedelius, G., 1875. *Hand-book for charcoal burners*. New York, NY: Wiley.
- Tarboton, D.G., 1997. A new method for the determination of flow directions and upslope areas in grid digital elevation models. *Water Resources Research*, 33 (2), 309–319. doi:[10.1029/96WR03137](https://doi.org/10.1029/96WR03137)
- Tarolli, P., Sofia, G., and Dalla Fontana, G., 2012. Geomorphic features extraction from high-resolution topography: landslide crowns and bank erosion. *Natural Hazards*, 61, 65–83. doi:[10.1007/s11069-010-9695-2](https://doi.org/10.1007/s11069-010-9695-2)
- Toffenetti, S., 1993. *I carbonai dell'Appennino*. Thesis. Università degli Studi di Bologna.
- Wilson, J.P. and Gallant, J.C., 2000. *Terrain analysis: principles and applications*. New York: John Wiley and Sons.
- Wood, J.D., 1996. *The geomorphological characterization of digital elevation models*. Thesis (PhD). University of Leicester.
- Wood, J.D., 2009b. Visualizing geomorphometry: lessons from information visualization. In: *Proceedings of geomorphometry*, 31 August–2 September 2009, Zurich.
- Wood, J.D., 2009a. *The LandSerf Manual*. London: City University.
- Zevenbergen, L.W. and Thorne, C.R., 1987. Quantitative analysis of land surface topography. *Earth Surface Processes and Landforms*, 12, 47–56. doi:[10.1002/esp.3290120107](https://doi.org/10.1002/esp.3290120107)